

In the format provided by the authors and unedited.

The impact of endothermy on the climatic niche evolution and the distribution of vertebrate diversity

Jonathan Rolland ^{1,2,3*}, Daniele Silvestro ^{1,2,4,5}, Dolph Schluter³, Antoine Guisan^{6,7}, Olivier Broennimann^{6,7} and Nicolas Salamin^{1,2}

¹Department of Computational Biology, Biophore, University of Lausanne, Lausanne, Switzerland. ²Swiss Institute of Bioinformatics, Quartier Sorge, Lausanne, Switzerland. ³Department of Zoology, University of British Columbia, Vancouver, Canada. ⁴Department of Biological and Environmental Sciences, University of Gothenburg, Gothenburg, Sweden. ⁵Gothenburg Global Biodiversity Centre, Gothenburg, Sweden. ⁶Department of Ecology and Evolution, Biophore, University of Lausanne, Lausanne, Switzerland. ⁷Institute of Earth Surface Dynamics, Geopolis, University of Lausanne, 1015 Lausanne, Switzerland. *e-mail: jonathan.rolland@yahoo.fr

31 **Supplementary methods and results**

32

33 Simulations of the ancestral states and quality of the estimates

34 We simulated a set of true ancestral states and we then tested whether our method could recover
35 accurately these states only with partial information (present day data and few/no fossils). These
36 tests are described in details in the supplementary material of Silvestro *et al.* 2017⁵² (the following
37 text has been modified from⁵²): For each simulation, we generated a complete phylogenetic tree
38 (extinct and extant taxa) under a constant rate of birth-death with 100 extant tips (using the
39 *sim.bd.taxa* function with parameters: speciation rate (λ) = 0.4, and extinction rate (μ) = 0.2, in the
40 R package TreePar⁵³). The number of fossils simulated on the tree was defined by a Poisson
41 distribution with expected number of occurrences set to 1, 5, and 20. Additional simulations were
42 also run without any fossils for comparison. The simulation under the model presented here
43 correspond to a constant rate of evolution σ^2 drawn from a gamma distribution $\Gamma(2, 5)$, and no
44 phenotypic trend ($\mu_0 = 0$). We simulated 100 data sets under each scenario (i.e. number of fossils
45 = 0, 1, 5, and 20). We analyzed each simulated dataset to estimate the rate parameters of the
46 Brownian Motion model (σ^2) and the ancestral states. Each dataset was run for 500,000 MCMC
47 generations, sampling every 500 steps. We summarized the results in two ways. First, we
48 numerically quantified the overall accuracy of the σ^2 estimate across all simulations using the mean
49 absolute percentage error (MAPE):

$$50 \quad MAPE_j(\sigma^2) = \frac{1}{N} \sum_{i=1}^N \left(\frac{|\hat{\sigma}_i^2 - \sigma_i^2|}{\sigma_i^2} \right)$$

51 where j is the simulation number, $\hat{\sigma}_i^2$ is the estimated rate at branch i , and σ_i^2 is the true rate at
52 branch i , and N is the number of branches in the tree. Secondly, we calculated the coefficient of

53 determination (R^2) between the true and the estimated ancestral states. These analyses showed that
54 our method is not biased (Supplementary Figure 8) and yields accurate estimations of ancestral
55 states (Supplementary Figure 9). Additional test on the performance of the method are described
56 in Silvestro *et al.* ⁵². The code used to run these simulations is available at:
57 <https://github.com/dsilvestro/fossilBM>.

58

59 Robustness of the results

60

61 To verify that our results were not affected by methodological biases, we ran a series of robustness
62 tests.

63 1. *Niche evolution estimates might be artificially high in mammals and birds because there*
64 *is more fossil data in these groups, or if the fossil record is biased (e.g if tropical*
65 *occurrences were less likely to be recorded in the fossil record)*. We ran all of the analyses
66 again without the fossils and found that niche evolution remained faster in
67 endotherms (Supplementary Figure 2). This latter result ensure that the main results of our
68 study will hold even if fossil occurrences might not reflect the true ancestral latitude of the
69 clades, and if fossils are misplaced on the tree (e.g. including changes in taxonomy between
70 the fossil record and the phylogeny).

71 2. *Niche evolution estimates might be artificially high in mammals and birds because these*
72 *two groups have larger phylogenies*. We ran all of the analyses again using pruned trees
73 for each group and found that niche evolution remained faster in endotherms
74 (Supplementary Figure 2).

75 3. *Niche evolution estimates might be artificially low in amphibians and squamates because*
76 *they are older groups.* We tested for a relationship between the estimates of niche evolution
77 rates in the 20 main orders (in birds and mammals) or families (in amphibians and
78 squamates) and their age and did not observe a significant relationship (Supplementary
79 Figure 6), which suggests that our results are not biased in this respect.

80 4. *Niche evolution estimates might be artificially high in mammals and birds because of our*
81 *evolution model.* We tested whether similar niche evolution estimates could be obtained
82 when applying Brownian motion (BM) and Ornstein-Uhlenbeck (OU) models (using the
83 *fitContinuous* R function in the *geiger* package). We obtained mean temperatures for each
84 species for which we had occurrence data points (GBIF), spatial distribution data (IUCN)
85 and mean annual temperature climatic layer data (BIO1, WorldClim), and we estimated
86 the rate of temperature evolution along the phylogenies for the four groups. These results,
87 which do not include fossil information, confirmed our previous results in which
88 endotherms were shown to have a faster niche evolution rate (Supplementary Table 1).

89 5. *Niche evolution estimates might be artificially high in birds because of migratory behavior.*
90 It is difficult to describe with confidence the distribution of migratory species, as their
91 occupancy area change across seasons. For birds, we estimated the niche evolution rate
92 based on the mean annual temperatures of both the breeding and wintering ranges (the
93 global distribution of each species without accounting for seasonal changes). This
94 simplification might affect our niche evolution reconstruction and we might have
95 underestimated the mean temperatures of migratory species; thus, we may have artificially
96 inflated the rate of niche evolution in birds. To test for this potential bias, we re-estimated
97 the rate of niche evolution using a BM model (using the *fitContinuous* R function in the

98 *geiger* package) that did not include fossil data but did include a phylogeny that only
99 contained sedentary species as well as the mean temperatures obtained for each species.
100 We also obtained migratory bird status data using the BirdLife International and
101 NatureServe databases (<http://www.birdlife.org/>). Following the method described in
102 Somveille *et al.*⁵⁴, we considered a species to be migratory if it has at least one non-
103 breeding season polygon or one breeding season polygon (see Rolland *et al.*⁵⁵ for more
104 details). We found migratory data for 6,142 of the species in our dataset, and we removed
105 1,387 migratory species, thus retaining a total of 4,755 sedentary species. We obtained
106 comparable BM estimates between the sedentary birds (e.g., BM $\sigma^2=9.05$) and all birds
107 (e.g., BM $\sigma^2=14.84$, Supplementary Table 1), suggesting that potential bias caused by using
108 mean annual temperatures does not affect our results and indicating that niche evolution
109 remains higher in birds than in the three other groups (Mammals BM $\sigma^2=2.92$, Amphibians
110 BM $\sigma^2=1.01$ and Squamates BM $\sigma^2=0.65$, Table S1).

111 6. *GBIF occurrence data points might be unevenly distributed inside the IUCN polygons and*
112 *lead to biased values of altitude, latitude and temperature.* If the occurrence points inside
113 the polygons were geographically (or environmentally) clustered, we would expect to see
114 a mismatch between data extracted from polygons alone and data extracted from
115 occurrences points inside the polygons. We thus extracted the latitude, altitude and
116 temperature values for each species from polygons alone and we then tested if there was a
117 considerable difference with the same data obtained from occurrences inside the polygons.
118 We found no systematic bias in the values extracted with both approaches and an extremely
119 high association between these variables (for latitude: $R^2_{\text{birds}} = 0.88$, $R^2_{\text{mammals}} = 0.97$,
120 $R^2_{\text{amphibians}} = 0.99$, $R^2_{\text{squamata}} = 0.99$; for altitude: $R^2_{\text{birds}} = 0.78$, $R^2_{\text{mammals}} = 0.8$, $R^2_{\text{amphibians}} = 0.86$,

121 $R^2_{\text{squamata}} = 0.83$; and for temperature: $R^2_{\text{birds}} = 0.82$, $R^2_{\text{mammals}} = 0.91$, $R^2_{\text{amphibians}} = 0.91$,
122 $R^2_{\text{squamata}} = 0.91$; $P < 10^{-16}$ for all groups). These results suggest that occurrences data are not
123 strongly biased and represent accurately the variation of ecological conditions contained
124 inside polygons.

125 7. *The temperature curve used in our study might be biased in the Neogene due to the*
126 *presence of ice volumes.* Our paleo-temperature curve is based on the deep-sea benthic
127 foraminiferal oxygen-isotope $\delta^{18}\text{O}$ (Zachos *et al.* ¹⁹). These estimates conflate temperature
128 and ice volume, which may be problematic when comparing greenhouse Eocene and
129 icehouse Neogene. We now run the analyses with two other Cenozoic curves from Cramer
130 *et al.* 2011 ⁵⁶ (based on formulas 7a and 7b in the supplementary information of the study)
131 that are based on the ratio Mg/Ca for the Cenozoic. In order to cover the 270 Myr of our
132 study, we did not change the temperature curve before 62.4 Myr, and the Cramer *et al.*
133 2011 ⁵⁶ curves were used after 62.4 Myr (we ran two independent analyses for the two
134 curves). We found no effect of these new curves on our results with faster rate of niche
135 evolution in birds and mammals compared to squamates and amphibians (birds= 0.86 or
136 0.64°C/Myr, respectively for the formulas 7a or 7b of Cramer *et al.* 2011 ⁵⁶, mammals=
137 0.70 or 0.52°C/Myr, amphibians= 0.37 or 0.31 °C/Myr, squamates= 0.40 or 0.33°C/Myr.

138 8. *We also tested whether branches leading to nodes or tips informed by fossil or present-day*
139 *data were giving the same results as the whole phylogeny.* This test permitted to test the
140 robustness of our phylogenetic approach. We found the same results with only branches
141 related to nodes informed by fossil or tips informed by field data, with higher rate of niche
142 evolution for endotherms than ectotherms (mean rate of niche evolution birds=

143 2.09°C/Myr, mammals= 2.37°C/Myr, amphibians= 0.56°C/Myr, squamates=
144 0.61°C/Myr).

145

146 **Supplementary references**

147 52. Silvestro D., Tejedor M. F., Serrano-Serrano M. L., Loiseau O., Rossier V., Rolland J.,
148 Zizka A., Antonelli A. & Salamin N. Evolutionary history of New World monkeys
149 revealed by molecular and fossil data. *BioRxiv* (2017) (available online at
150 <http://www.biorxiv.org/content/early/2017/08/18/178111.article-metrics>).

151 53. Stadler, T. Mammalian phylogeny reveals recent diversification rate shifts. *Proc. Natl.*
152 *Acad. Sci. U.S.A.* **108** , 6187-6192 (2011).

153 54. Somveille, M., Manica, A., Butchart, S. H. & Rodrigues, A. S. Mapping global diversity
154 patterns for migratory birds. *PLOS ONE* **8**, e70907 (2013).

155 55. Rolland, J., Jiguet, F., Jønsson, K. A., Condamine, F. L. & Morlon, H. Settling down of
156 seasonal migrants promotes bird diversification. *Proc. Biol. Sci.* **281**, 20140473 (2014).

157 56. Cramer, B. S., Miller, K. G., Barrett, P. J., & Wright, J. D. Late Cretaceous–Neogene trends
158 in deep ocean temperature and continental ice volume: Reconciling records of benthic
159 foraminiferal geochemistry ($\delta^{18}\text{O}$ and Mg/Ca) with sea level history. *J. Geophys. Res*
160 *Oceans.* **116**. (2011).

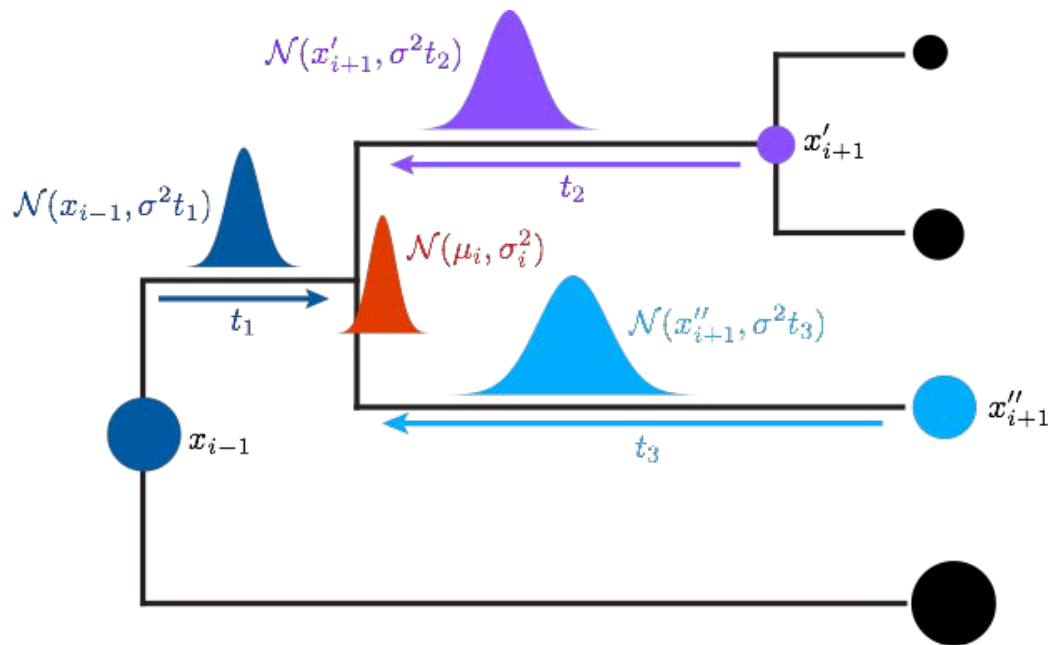
161

162

163

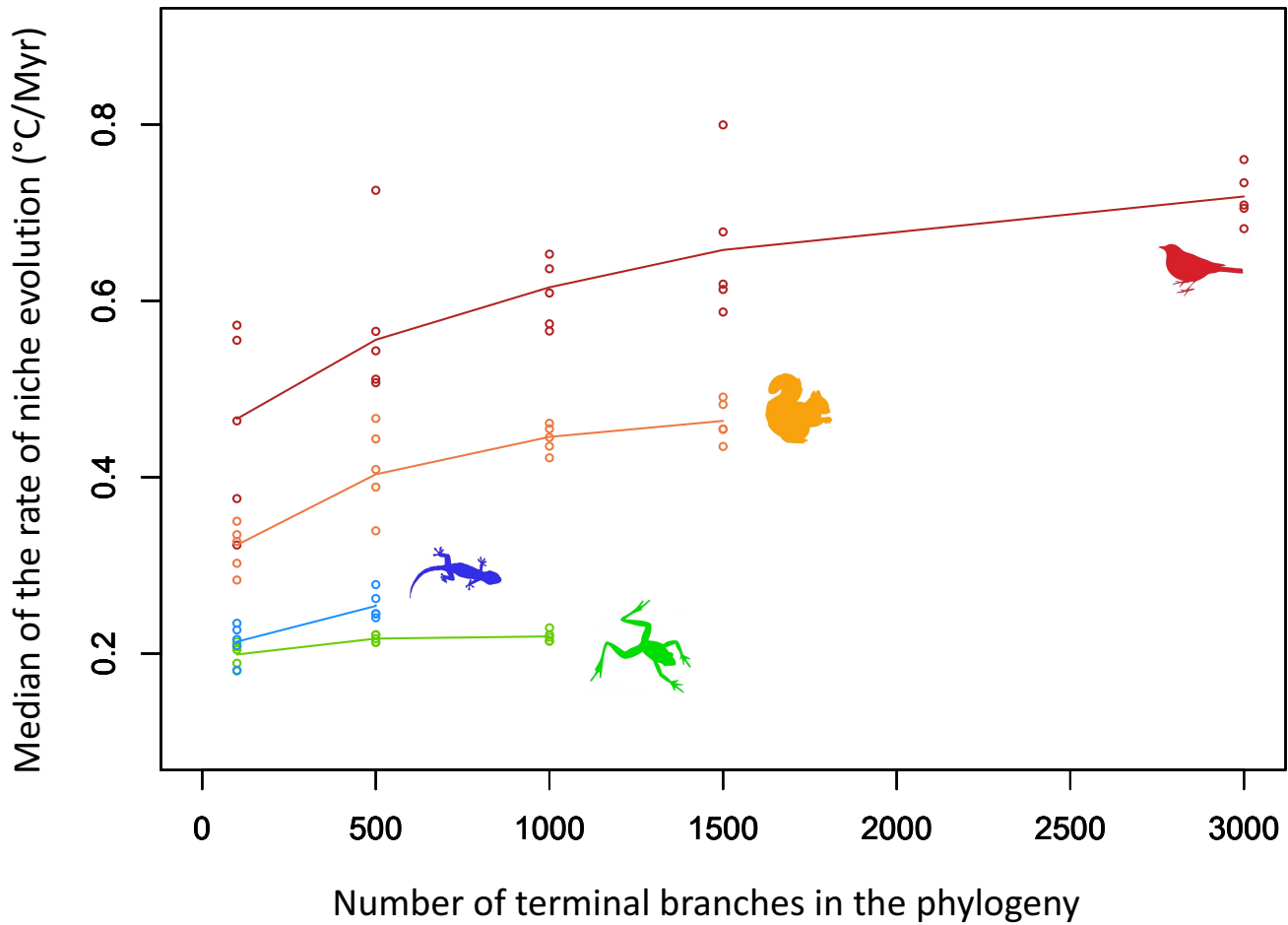
164

165

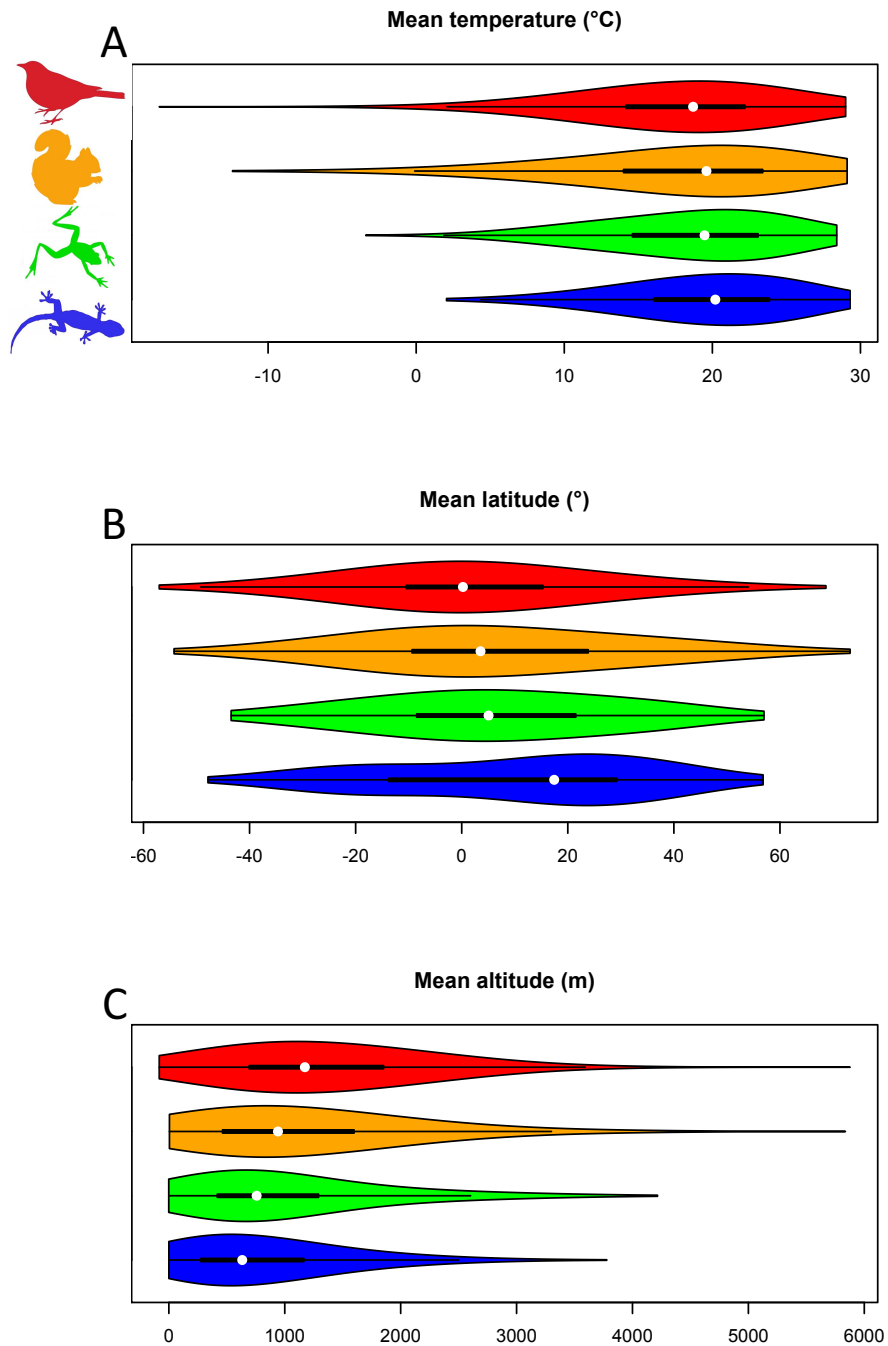


166

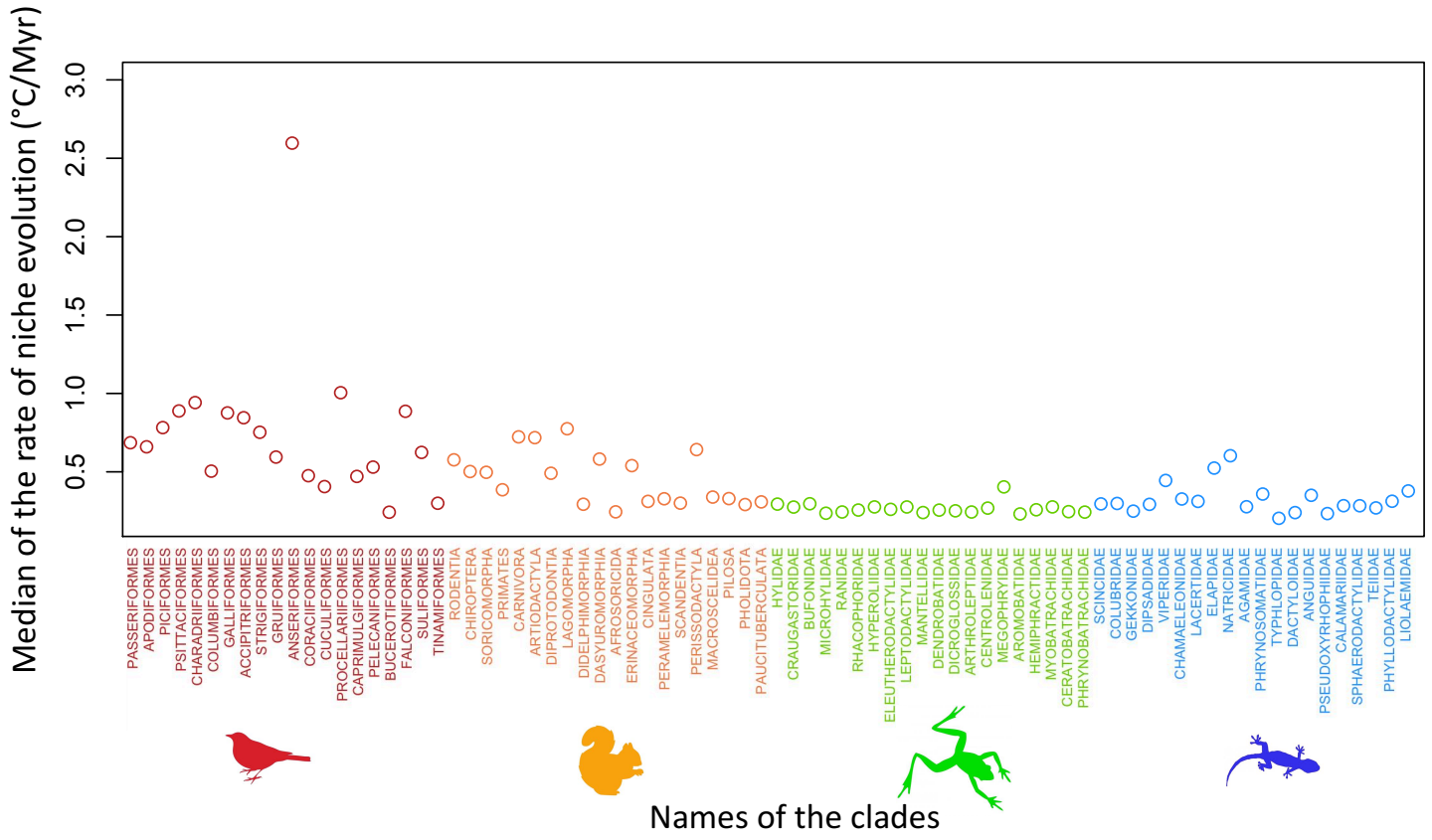
167 **Supplementary Figure 1. Bayesian inference of ancestral states using a fossil-calibrated**
 168 **Brownian motion model of evolution.** The example shows an ultrametric tree with trait values
 169 indicated by the size of the circles at the tips and at the internal nodes. The ancestral state of any
 170 given internal node i is sampled directly from its joint posterior distribution through Gibbs
 171 sampling. The joint posterior distribution of node i is a normal distribution obtained by combining
 172 four normal distributions: three from the expectation of the Brownian motion with rate parameter
 173 σ^2 (ancestral node in dark blue and the two descendant values in purple and light blue) and one for
 174 the prior assigned to the node (in red). The prior is either informative, i.e. when defined based on
 175 fossil data, or non-informative with an arbitrary large variance if fossils are not available (see
 176 "Fossils" and "Ancestral reconstruction of latitude and altitude" sections for more details).



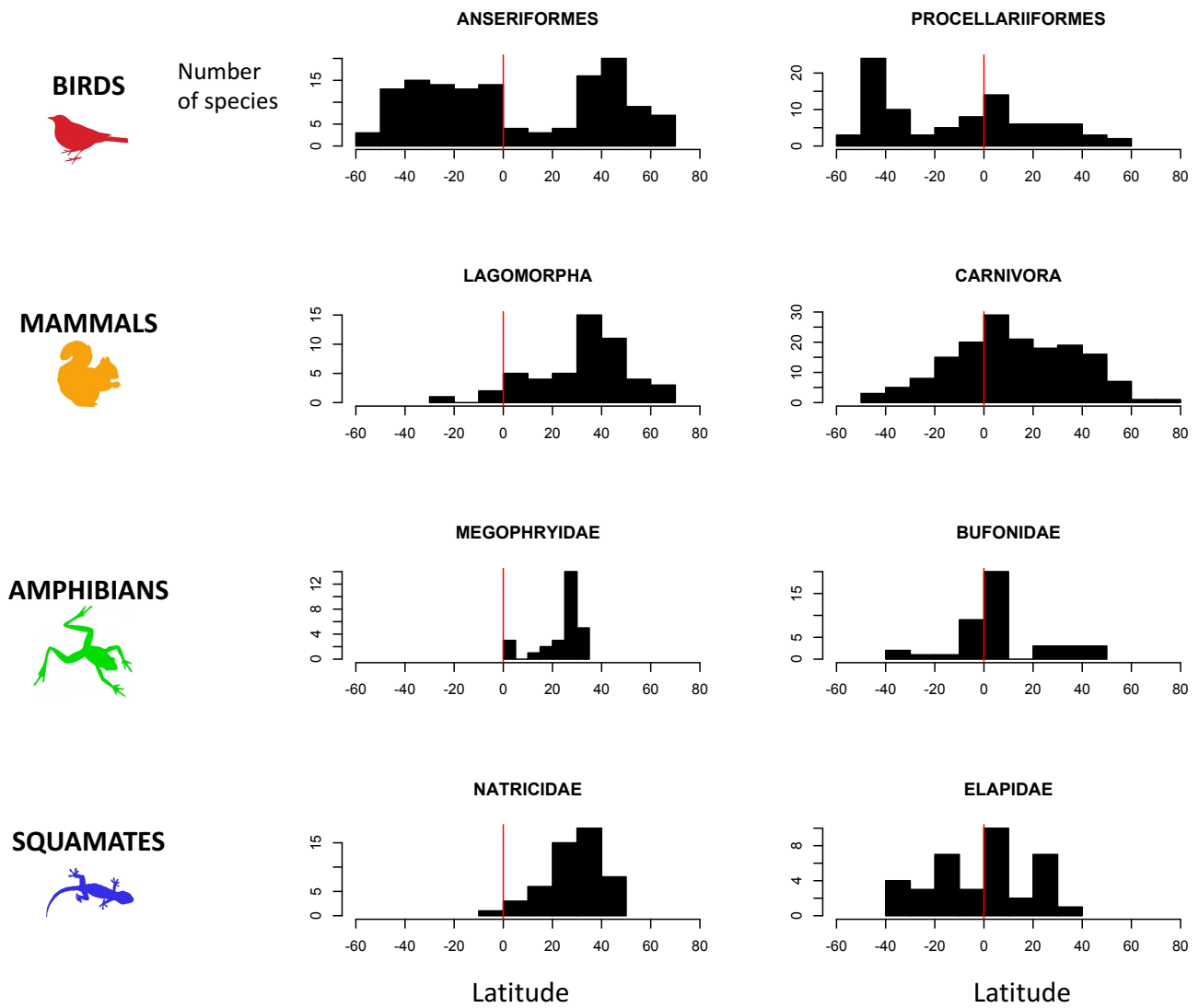
178 **Supplementary Figure 2. Robustness analysis. Niche evolution remains faster in endotherms**
 179 **even when trees are pruned and fossil data are removed.** The niche evolution of each group
 180 was estimated based on four reconstructions: minimum and maximum latitude and minimum and
 181 maximum altitude. These four analyses were run on trees of five different sizes for birds (3000,
 182 1500, 1000, 500 and 100 tips), four different sizes for mammals (1500, 1000, 500 and 100 tips),
 183 three different sizes for amphibians (1000, 500 and 100 tips), and two different sizes for squamates
 184 (500 and 100 tips). Each reconstruction was replicated five times for each tree size, for a total of
 185 $5 \times 4 \times 14 = 280$ reconstructions. We designed a pruning algorithm to remove randomly
 186 monophyletic clades from the original tree (code available at
 187 https://github.com/jonathanrolland/niche_evolution). This methodology allowed us to retain the
 188 phylogenetic signal inside each group and was more conservative than randomly pruning
 189 individual tips (rates of niche evolution were substantially higher when the tips were randomly
 190 removed). In addition, to account for the potential effect of fossils in our results, we did not
 191 consider fossil information in these robustness analyses.
 192



193
 194 **Supplementary Figure 3. Avian (red) and mammalian (orange) species cover a wider range**
 195 **of mean temperature, mean latitude and mean altitude than amphibian (green) and**
 196 **squamate (blue) species. Violin plots were calculated using all of the species in each group.**



198 **Supplementary Figure 4. Median rate of niche evolution for the 20 richest orders of birds**
 199 **(red) and mammals (orange) and the 20 richest families of amphibians (green) and**
 200 **squamates (blue).**



201
 202 **Supplementary Figure 5. Latitudinal diversity gradients of the groups that showed rapid**
 203 **niche evolution.** The vertical red line corresponds to the equator.

204

205

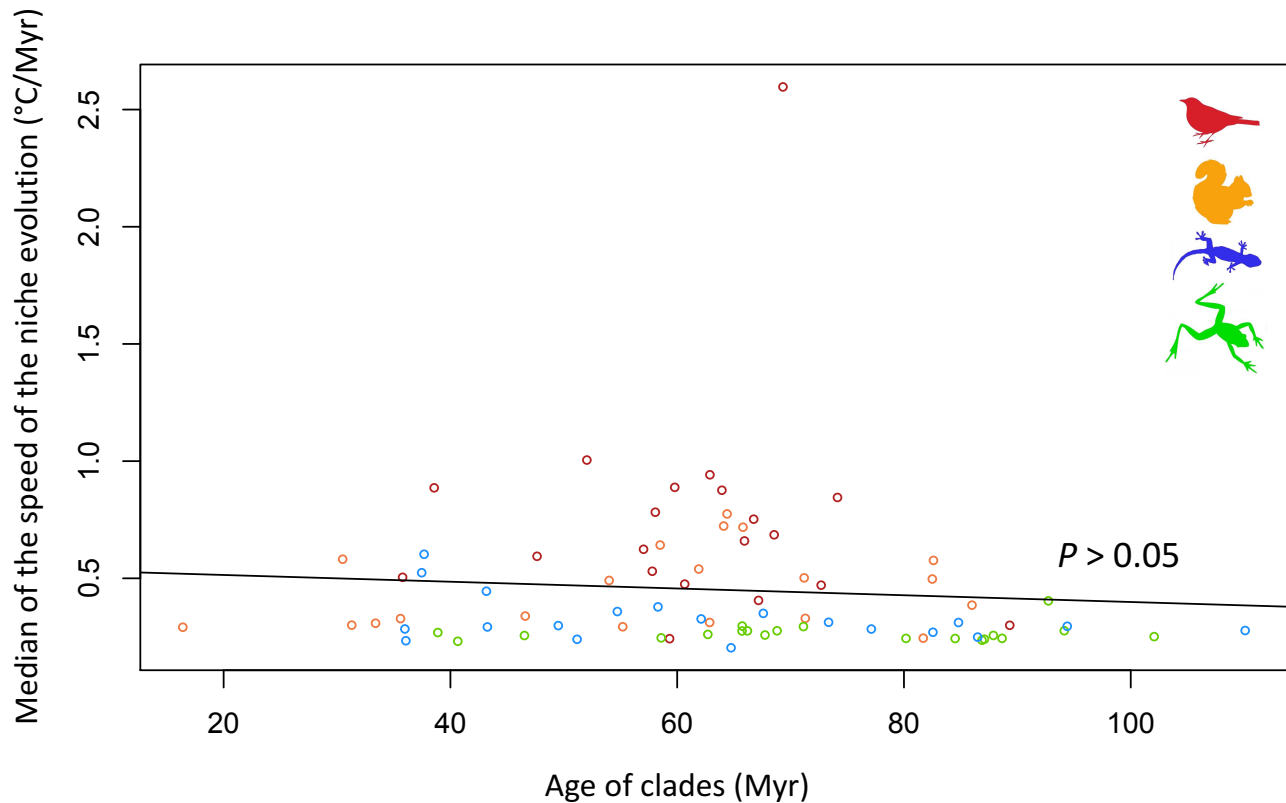
206

207

208

209

210



211

212 **Supplementary Figure 6. Robustness analysis. Niche evolution rates are not associated with**
 213 **the age of the clades (orders and families).** The rate of niche evolution was estimated for the 20
 214 richest orders of birds (red) and mammals (orange) and the 20 richest families of amphibians
 215 (green) and squamates (blue). The black line represents the regression of the linear model between
 216 the rate of niche evolution and the age of the groups ($P > 0.05$).

217

218

219

220

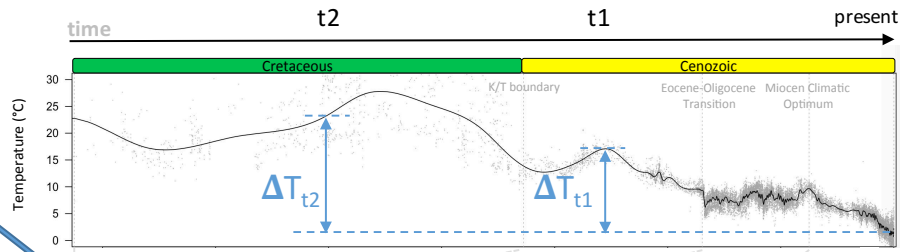
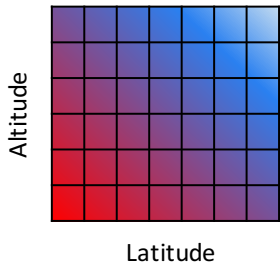
221

222

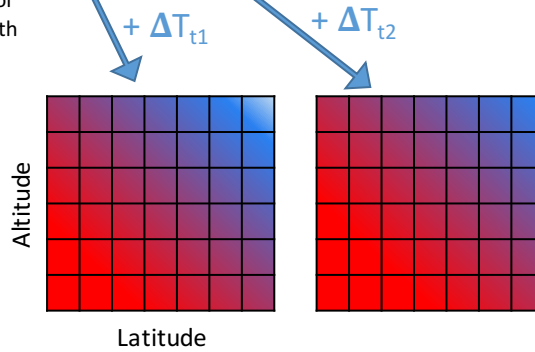
223

224

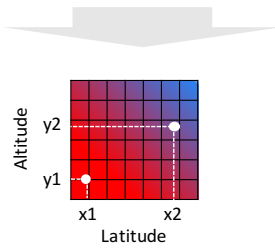
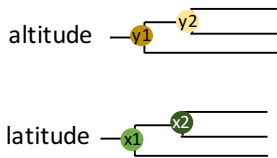
1 The first grid is calculated from temperature layers at present



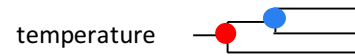
2 Rescaling all the values of the temperature grid with the delta temperature between t and present



3 Reconstruct altitude and latitude preferences on phylogenies



4 Determine the temperature corresponding to the latitude-altitude combination of each node for the grid built at the age of the node.



225

226 **Supplementary Figure 7. Description of the procedure to obtain temperature for each node**
 227 **of the phylogeny from both the reconstructions of latitude and altitude and the climatic grid**
 228 **through time.**

229

230

231

232

233

234

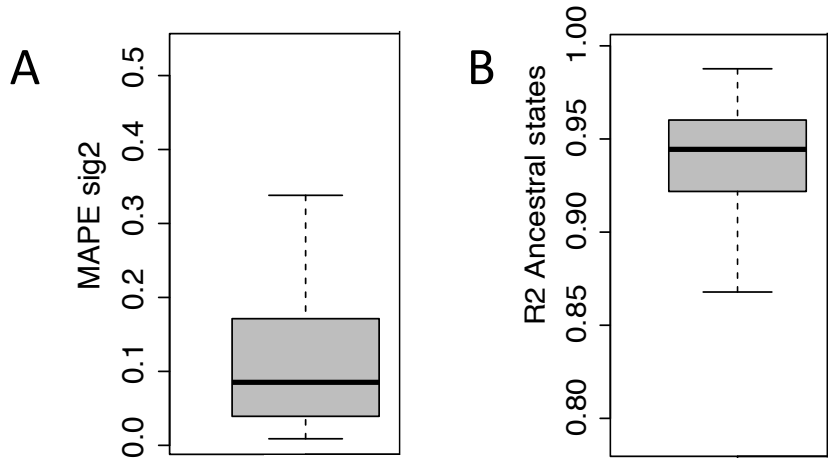
235

236

237

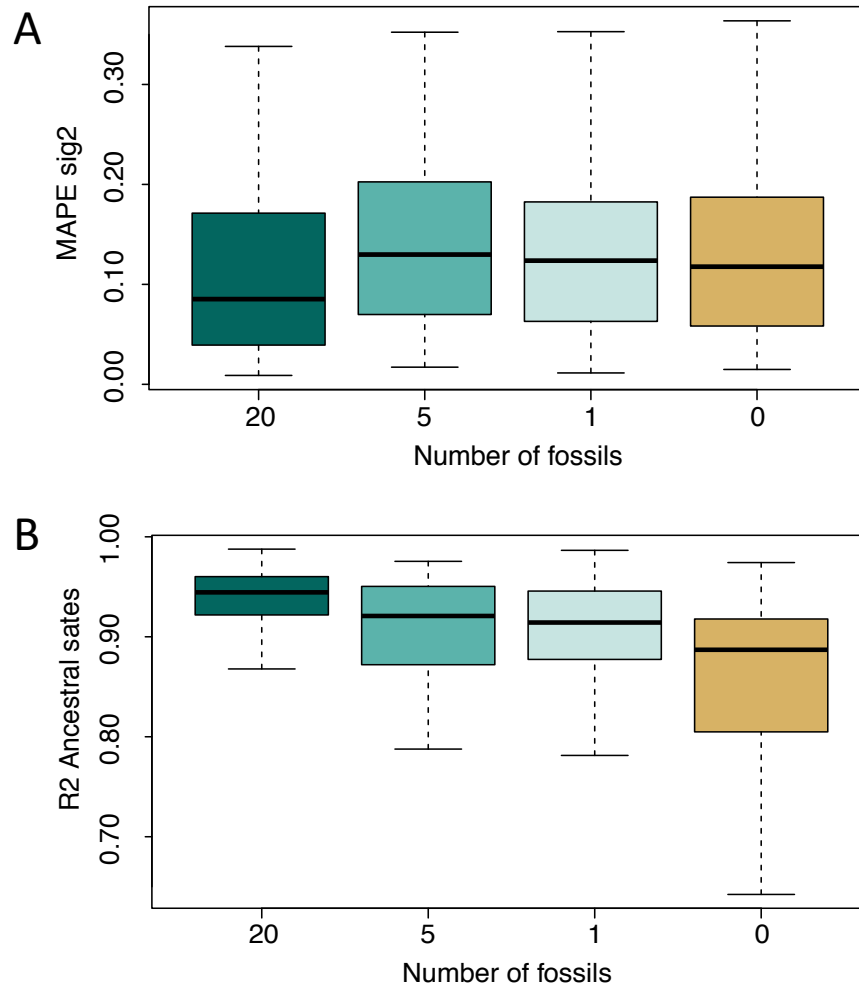
238

239



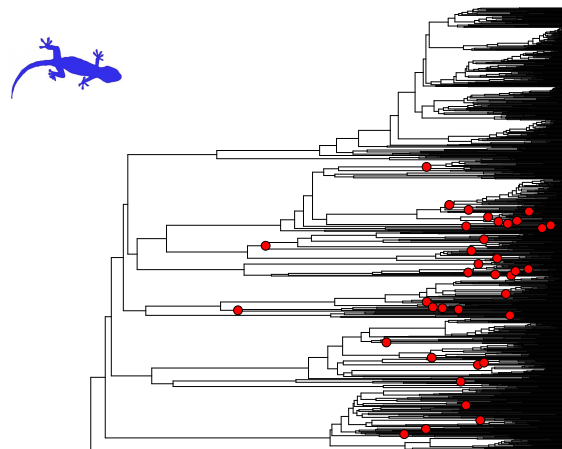
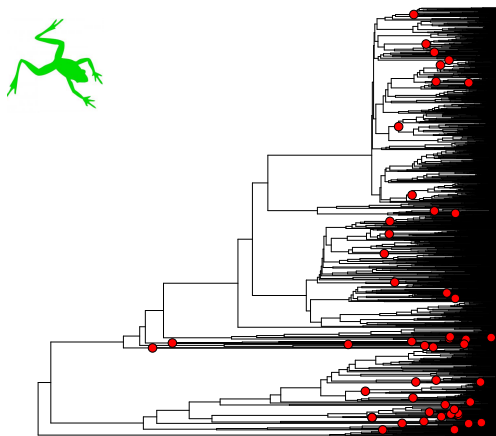
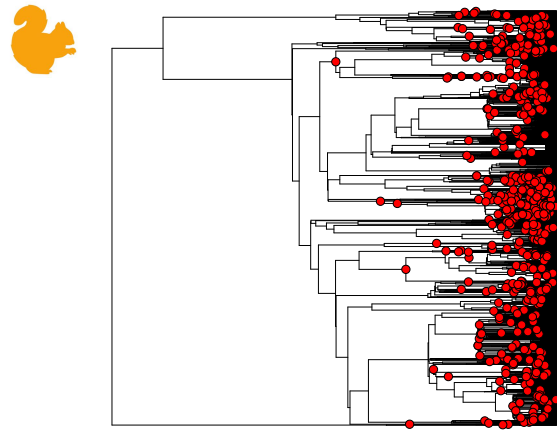
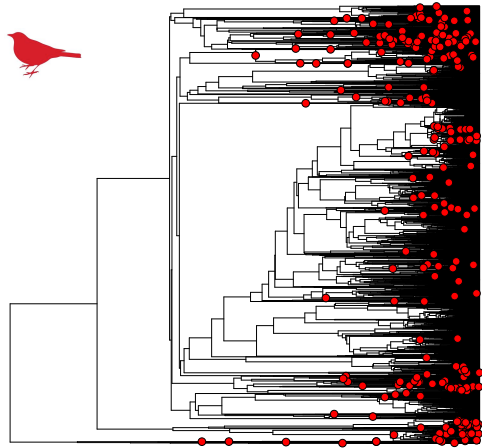
240
241
242
243
244
245
246
247

Supplementary Figure 8. Accuracy of parameter estimation summarized across 100 simulations. Mean absolute percentage errors (MAPE) are reported for the rate parameters (σ^2 , panel A), and the coefficient of determination is used for ancestral states (R^2 , panel B, modified from Figure S2 of Silvestro *et al.* 2017⁵²).



248
 249
 250
 251
 252
 253
 254
 255
 256
 257
 258
 259
 260
 261
 262
 263
 264
 265

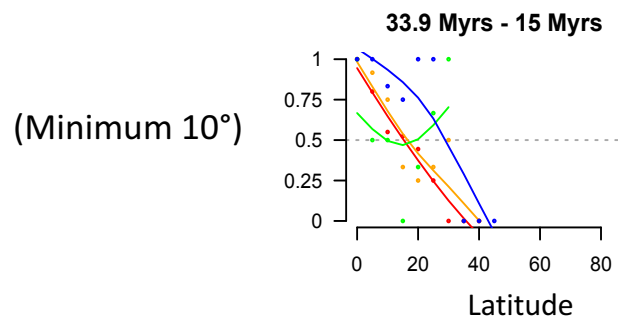
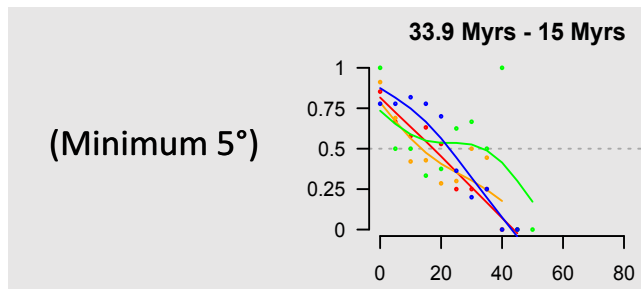
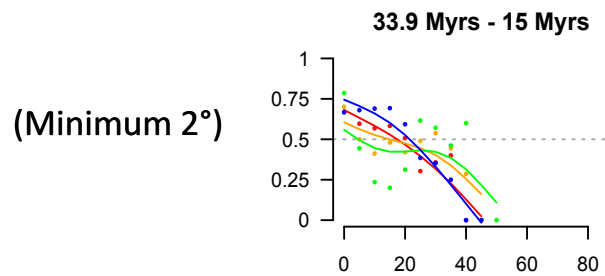
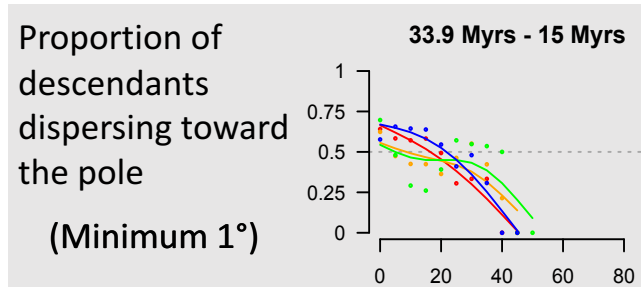
Supplementary Figure 9. Accuracy of parameter estimation summarized across 100 simulations with decreasing number of fossils: 20, 5, 1, and 0. Mean absolute percentage errors (MAPE) are reported for the rate parameters (σ^2 , panel A), and the coefficient of determination R^2 is used for ancestral states (R^2 , panel B). (modified from Figure S3 of Silvestro *et al.* 2017⁵²).



266
 267
 268
 269
 270
 271
 272
 273
 274
 275
 276
 277
 278
 279
 280
 281
 282
 283
 284
 285
 286

Supplementary Figure 10. Distribution of the nodes calibrated using fossil information (red points) on the phylogenies of the four studied groups. 2663 fossil occurrences were used to calibrate 239 of the 6141 nodes present in the birds phylogeny, 21767 fossil occurrences were used to calibrate 473 or the 2921 nodes of the mammals phylogeny, 908 occurrences were used to calibrate 48 of the 1413 nodes in amphibian phylogeny and 476 occurrences permitted to calibrate 37 of the 986 nodes in squamates phylogeny, the rest of the nodes in the phylogenies had flat priors. We also provided in Table S2-S4 the number of fossils that permitted to calibrate each node.

287
288



289
290
291
292
293
294
295
296
297

Supplementary Figure 11. Robustness analysis. The pattern of the dispersal of the species distributed at high latitudes towards the equator (presented in the figure 3D) is robust when we considered only the lineages that disperse more than 1°, 2°, 5° or 10° latitude.

298 **Supplementary Table 1. Robustness analysis. Niche evolution rates remain higher in birds**
 299 **and mammals when estimated based on Brownian motion (BM) and Ornstein-Uhlenbeck**
 300 **(OU) models and when the present time mean annual temperatures are used for each species**
 301 **(BIO1 from WorldClim).** This analysis was performed using the *fitContinuous* function in the
 302 *geiger* R package. z_0 corresponds to the ancestral value of temperature at the root of the tree
 303 according to the BM process, and α measures the strength of attraction of the OU process toward
 304 the point of attraction θ . Compared with previous analyses, ancestral temperatures were not
 305 estimated using latitudinal and altitudinal reconstructions. This analysis did not include fossil data.

	Brownian motion			Ornstein–Uhlenbeck			
	AIC	σ^2	z_0	AIC	σ^2	α	θ
Birds	47361.6	14.84	19.47	39728.1	206.81	2.72	19.20
Mammals	19018.6	2.92	18.87	18439.5	4.56	0.047	19.08
Amphibians	9047.5	1.01	16.39	8601.2	1.61	0.024	17.69
Squamates	5760.5	0.65	21.25	5600.5	1.08	0.022	20.97

306
 307
 308
 309
 310
 311
 312
 313
 314
 315
 316
 317
 318
 319

320 **Supplementary Table 2. Number of fossil occurrences used to inform the most recent**
 321 **common node of each genus in the birds phylogeny.**

Birds							
Genus	Nb. of fossils used to inform the node						
Aythya	38						
Anas	165	Perisoreus	3	Streptopelia	4	Gallirallus	3
Crinifer	1	Melospiza	6	Aegypius	2	Chenonetta	2
Nycticorax	8	Circus	5	Milvus	3	Pelecanoides	5
Pandion	10	Molothrus	6	Tadorna	9	Cyanoramphus	2
Haliaeetus	14	Cardinalis	4	Caprimulgus	2	Eudiptes	5
Meleagris	45	Zonotrichia	12	Oceanites	4	Coenocorypha	2
Spheniscus	18	Accipiter	25	Colius	4	Apteryx	2
Phalacrocorax	80	Melanerpes	15	Pachyptila	8	Megadyptes	3
Fulmarus	11	Passerina	1	Scopus	1	Hemiphaga	2
Sula	34	Junco	8	Leptoptilos	8	Anthornis	1
Buteo	70	Zenaida	21	Turnix	6	Thalassarche	2
Gavia	40	Colaptes	27	Passer	1	Petroica	1
Morus	29	Passerculus	4	Ploceus	2	Hymenolaimus	1
Puffinus	69	Tyto	33	Coturnix	13	Coracopsis	1
Diomedea	9	Passerella	2	Ephippiorhynchus	2	Leptopterus	1
Uria	21	Picoides	6	Hirundo	8	Foudia	1
Cepphus	6	Aphelocoma	4	Carduelis	6	Upupa	1
Oceanodroma	2	Podiceps	28	Gypaetus	1	Terpsiphone	1
Dromaius	10	Vermivora	2	Athene	11	Mirafr	1
Calonectris	6	Coragyps	16	Parus	3	Zosterops	1
Ortalis	4	Columba	24	Jabiru	4	Oreortyx	3
Tympanuchus	10	Bubo	33	Alauda	7	Loxia	3
Strix	17	Sturnella	11	Eremophila	8	Bombycilla	1
Geranoaetus	5	Coccyzus	4	Sturnus	11	Menura	1
Ardea	31	Glaucidium	4	Otis	4	Brachyramphus	2
Burhinus	5	Euphagus	6	Surnia	5	Rissa	3
Mycteria	10	Asio	20	Apus	3	Aegothales	1
Grus	33	Dryocopus	4	Gallus	9	Collocalia	1
Aramus	5	Tachybaptus	2	Pyrrhocorax	11	Cinlosoma	2
Balearica	2	Hylocichla	2	Casuaris	1	Ptilonorhynchus	1
Anhinga	16	Ammodramus	3	Cerorhinca	6	Cacatua	2
Egretta	14	Buteogallus	3	Synthliboramphus	12	Anthochaera	2
Ardeola	1	Cyanocitta	12	Alca	25	Phaps	2
Jacana	4	Porzana	21	Aethia	4	Dasyornis	2
Phoenicopteris	10	Turdus	46	Haematopus	7	Glossositta	1
Fulica	27	Dumetella	2	Pluvialis	7	Platycercus	1
Bartramia	5	Chondestes	2	Bulweria	1	Phalaropus	2
Falco	62	Toxostoma	4	Fratercula	15	Neochen	1
Aquila	23	Catharus	3	Procellaria	2	Pagophila	1
Ptychoramphus	9	Spizella	6	Sterna	3		
Mergus	29	Calidris	13	Pterodroma	9		
Ceryle	1	Cathartes	16	Chloephaga	3		
Podilymbus	31	Aegolius	8	Rhea	10		
Corvus	82	Quiscalus	9	Nothura	2		
Agelaius	15	Pica	10	Pygocelis	4		
Rallus	38	Recurvirostra	5	Vultur	2		
Aix	8	Somateria	8	Sarcoramphus	2		
Bucephala	13	Pelecanus	9	Eudromia	2		
Limnodromus	6	Charadrius	12	Columbina	4		
Colinus	24	Cistothorus	3	Milvago	4		
Butorides	6	Caracara	17	Arenaria	4		
Ciconia	19	Pipilo	4	Crypturellus	1		
Gallinula	13	Icterus	2	Syrigma	1		
Spizaetus	4	Anser	24	Thinocorus	3		
Gymnogyps	18	Xanthocephalus	3	Theristicus	1		
Gallinago	7	Tachycineta	4	Alle	18		
Botaurus	8	Lophodytes	7	Dendragapus	5		
Laterallus	5	Numenius	13	Cyrtonyx	3		
Nyctanassa	6	Cygnus	17	Callipepla	1		
Tringa	13	Melanitta	12	Pavo	1		
Dendrocygna	8	Stercorarius	6	Sayornis	4		
Scolopax	14	Larus	36	Petrochelidon	2		
Ixobrychus	3	Aechmophorus	5	Contopus	2		
Eudocimus	12	Megaceryle	3	Sitta	5		
Branta	34	Dendrocopos	4	Phaethon	1		
Oxyura	3	Limosa	7	Carpodacus	3		
Plegadis	4	Struthio	72	Chaetura	2		
Otus	21	Francolinus	28	Pinicola	2		
Bonasa	12	Numida	14	Piranga	2		

323 **Supplementary Table 3. Number of fossil occurrences used to inform the most recent**
 324 **common node of each genus in the mammals phylogeny.**

		Arctonyx	9	Desmodus	16	Dasyprocta	6	Mystromys	21	Leopoldamys	3	Natalus	1
		Cuon	16	Pan	2	Marmosa	14	Malacothrix	7	Petromus	1	Mogera	3
		Rattus	34	Hydrochoerus	19	Tamandua	4	Sylvicapra	6	Gerbillurus	1	Pteromys	1
		Eothenomys	2	Mormoops	5	Choloepus	3	Dendrohyrax	5	Lagostomus	28	Hylobates	1
		Viverra	24	Pongo	16	Antidorcas	146	Myoprocta	2	Oryctolagus	58	Myocastor	15
		Giraffa	252	Trachypithecus	7	Litocranius	3	Potos	3	Nesokia	7	Chaetophractus	16
		Lutra	42	Macropus	94	Aepyceros	146	Caluromys	4	Thamnomys	3	Zaedyus	12
		Tapirus	246	Dasyurus	10	Damaliscus	131	Monodelphis	2	Miniopterus	21	Microcavia	10
		Potamochoerus	60	Boselaphus	1	Connochaetes	158	Metachirus	4	Grammomys	1	Lestodelphys	7
		Moschus	9	Bison	263	Hippotragus	76	Ateles	3	Atelerix	3	Akodon	7
		Muntiacus	34	Rangifer	76	Oryx	41	Chirotopes	1	Zelotomys	8	Oxymycterus	3
		Crocidura	145	Redunca	116	Kobus	321	Pithecia	1	Zenkerella	2	Reithrodon	13
		Blarinella	10	Atlantoxerus	26	Madoqua	27	Mesomys	2	Rousettus	8	Phyllotis	7
		Anourosorex	8	Sciurus	104	Otocyon	12	Proechimys	8	Neotragus	2	Galea	8
		Myotis	231	Ochotona	117	Mellivora	44	Philander	4	Crossarchus	2	Holochilus	11
		Eptesicus	73	Sicista	43	Papio	83	Bradypus	3	Scutisorex	2	Ozotoceros	6
		Pipistrellus	31	Apodemus	313	Pedetes	11	Prionodontes	2	Heliosciurus	1	Calomys	10
		Plecotus	34	Micromys	37	Thryonomys	43	Neacomys	1	Bdeogale	1	Lophostoma	1
		Callosciurus	5	Chironectes	3	Caracal	41	Rhipidomys	2	Funisciurus	2	Leptonycteris	2
		Tamias	3	Aotus	3	Ichneumia	8	Mazama	22	Protoxerus	2	Chimarrogale	2
		Dremomys	6	Presbytis	1	Cephalophus	59	Petaurides	2	Nyctereutes	41	Murina	4
		Hylapetes	12	Manis	10	Phacochoerus	90	Melomys	2	Anomalurus	1	Ptaurista	3
		Mus	61	Thylamys	7	Lycaon	17	Antechinus	10	Macroscelides	3	Chiropodomys	1
		Hystrix	203	Noctilio	5	Theropithecus	179	Planigale	1	Meriones	22	Burramys	2
		Macaca	70	Thyroptera	3	Mungos	9	Sminthopsis	8	Glis	73	Pseudochirops	2
		Martes	66	Leopardus	15	Loxodonta	137	Lagorchestes	2	Cricetus	94	Macroderma	2
		Felis	174	Lutreolina	6	Ceratotherium	205	Thylagale	4	Calomyscus	3	Dendrolagus	2
		Sus	182	Lepus	301	Diceros	96	Petaurus	4	Eliomys	106	Euphractus	7
		Rhinoceros	85	Basariscus	45	Tragelaphus	391	Cercartetus	1	Phascogale	2	Andinomys	2
		Gazella	424	Perognathus	136	Tatera	46	Aepyprymus	6	Sarcophilus	7	Euryzgomatmys	1
		Antelope	86	Spermophilus	388	Cercocebus	11	Bettongia	5	Phascolarctus	6	Hippocamelus	4
		Equus	1578	Catagonus	15	Syncerus	111	Wallabia	3	Vombatus	6	Graomys	1
		Hippopotamus	452	Thomomys	207	Genetta	33	Isoodon	3	Lasiurhinus	2	Balantiopteryx	1
		Cervus	399	Onychomys	61	Rhynchocyon	8	Perameles	8	Potorous	4	Liomys	3
		Capreolus	80	Antrozous	22	Civettictis	4	Pseudocheirus	5	Nyctophilus	1	Dolichotis	5
		Erinaceus	73	Geomys	171	Raphicerus	110	Trichosurus	12	Mastacomys	2	Blastocerus	2
		Hyaena	85	Ammospermophilus	20	Cercopithecus	25	Hydromys	2	Hypsigrymodon	1	Lyncodon	1
		Canis	713	Lasiurus	28	Colobus	11	Uromys	1	Strigoscopus	3	Pteronotus	3
		Vulpes	234	Parascalops	19	Aethomys	41	Pteronura	3	Muscardinus	61	Chrotopterus	1
		Ursus	346	Baiomys	25	Aonyx	26	Bassaricyon	2	Desmana	61	Lonchophylla	1
		Panthera	329	Nasua	7	Arvicanthus	22	Callicebus	1	Episoriculus	42	Necomys	3
		Microtus	816	Taxidea	62	Thallomys	27	Lagotherix	1	Meles	52	Lagidium	4
		Capra	41	Cynomys	85	Chlorocebus	12	Saguinus	3	Talpa	210	Colomys	1
		Bos	158	Scapanus	49	Scotophilus	4	Saimiri	1	Lagurus	36	Kerodon	1
		Procapra	83	Cryptotis	41	Nycteris	4	Dactylops	1	Urotrichus	10	Vicugna	1
		Hipposideros	31	Neurotrichus	3	Jaculus	5	Oecomys	2	Spalax	32	Aplodontia	5
		Rhinolophus	81	Tayassu	31	Mastomys	21	Oligoryzomys	4	Soriculus	7	Pappogeomys	2
		Tadarida	29	Cerdocyon	6	Xerus	16	Nectomys	2	Galemys	14	Solenodon	1
		Dasylops	83	Notiosorex	23	Taphozous	6	Marmosops	1	Neomys	20	Macrotytus	3
		Tamias	63	Reithrodontomys	85	Helogale	10	Callithrix	1	Dryomys	8	Brachyphylla	3
		Didelphis	44	Cratogeomys	22	Gerbillus	30	Dinomys	1	Cricetulus	27	Nycticeius	2
		Sylvilagus	275	Eumops	11	Pelomys	9	Alcelaphus	126	Arvicola	92	Geogale	2
		Blarina	82	Histiotis	1	Acomys	10	Acinonyx	28	Hemirragus	23	Microgale	6
		Scalopus	55	Dipodomys	135	Heterocephalus	14	Cabassous	1	Mesocricetus	5	Tenrec	2
		Sorex	516	Erethizon	66	Paraxerus	11	Microsciurus	1	Chionomys	2	Pteropus	1
		Marmota	104	Chrysocyon	5	Lemniscomys	14	Dasymys	16	Vormela	3	Microcebus	2
		Castor	172	Antilocapra	29	Myosorex	12	Lophuromys	2	Axis	8	Cheirogaleus	2
		Oryzomys	40	Orthogeomys	7	Suncus	23	Praomys	24	Myospalax	12	Lemur	2
		Peromyscus	309	Phenacomys	61	Eidolon	2	Cricetomys	4	Rupicapra	4	Propithecus	2
		Sigmodon	201	Lasionycteris	3	Galago	12	Graphiurus	12	Hemiechinus	1	Avahi	1
		Neotoma	318	Microdipodops	3	Heterohyrax	8	Sylvisorex	3	Barbastella	4	Fossa	1
		Neofiber	37	Oreamnos	9	Heteromys	3	Hylcocheirus	6	Nyctalus	3	Cryptoprocta	1
		Ondatra	162	Myodes	124	Eira	4	Ictonyx	7	Rhizomys	10	Nesomys	1
		Synaptomys	73	Chaetodipus	22	Gallictis	3	Proteles	9	Allactaga	8	Echinops	1
		Zapus	39	Ovis	90	Molossops	2	Cryptomys	22	Dorcopsis	3	Triaeops	1
		Urocyon	53	Enhydra	22	Molossus	3	Cynictis	18	Viverricula	1	Mormopterus	1
		Tremarctos	26	Lemmus	41	Artibeus	5	Elephantulus	32	Atherurus	3	Eliurus	2
		Procyon	92	Lemmings	28	Carollia	1	Amblysomus	6	Asellia	1	Paradoxurus	1
		Mustela	231	Brachylagus	8	Glossophaga	2	Steatomys	20	Tarsius	3	Uropus	1
		Spilogale	63	Ochrotomys	7	Micronycteris	4	Dendromus	21	Megaderma	8	Tylonycteris	1
		Megphitis	48	Glaucomys	26	Phyllostomus	3	Saccostomus	32	Ctenomys	27	Trichys	1
		Conepatus	19	Podomys	11	Sturnira	2	Otomys	34	Scaptonyx	5	Elaphodus	1
		Lontra	32	Tamiasciurus	33	Trachops	2	Rhabdomys	8	Alticola	1	Budorcas	1
		Lynx	161	Alces	50	Rhogeessa	2	Atilax	14	Eolagus	4	Phyllops	1
		Odocoileus	237	Condylura	12	Alouatta	5	Bathyergus	18	Cavia	9	Gracilinanus	2
		Puma	51	Napaeozapus	9	Cuniculus	8	Suricata	7	Hylomys	5	Scapteromys	2
		Hydropotes	5	Vespertilio	10	Rhynchonycteris	1	Georchus	3	Ratufa	4	Clyomys	1
		Elephas	85	Gulo	22	Tonatia	2	Parotomys	2	Tupaia	3	Thrichomys	1
		Crocota	142	Myrmecophaga	5	Cebus	4	Chrysochloris	8	Nycticebus	1	Prionailurus	1
		Paguma	4	Dicrostonyx	27	Zygodontomys	4	Tachyoryctes	15	Belomys	2	Lutrogale	1
		Herpestes	62	Ovibos	37	Coendou	8	Poecilogale	1	Niwiventer	7	Babyrousa	2

326 **Supplementary Table 4. Number of fossil occurrences used to inform the most recent**
 327 **common node of each genus in the amphibians and squamates phylogenies.**

Squamata		Amphibians	
Genus	Nb. of fossils used to inform the node	Genus	Nb. of fossils used to inform the node
Ophisaurus	107	Salamandra	20
Uromastyx	4	Pelodytes	6
Sceloporus	42	Plethodon	7
Anolis	25	Rana	212
Gerrhonotus	12	Pseudotriton	1
Rhineura	11	Bufo	195
Leiocephalus	7	Ambystoma	96
Eumeces	38	Hyla	64
Holbrookia	10	Barbourula	1
Phrynosoma	25	Tylototriton	2
Heloderma	4	Necturus	2
Crotaphytus	13	Cryptobranchus	8
Gambelia	1	Amphiuma	9
Uta	1	Siren	30
Anniella	2	Scaphiopus	28
Varanus	35	Rhinophrynus	2
Egernia	2	Taricha	3
Blanus	13	Spea	32
Chalcides	8	Andrias	13
Trogonophis	1	Acris	10
Lacerta	82	Pseudacris	21
Tarentola	3	Pseudobranchus	5
Agama	3	Notophthalmus	12
Tropidophorus	2	Gyrinophilus	3
Chamaeleo	8	Gastrophryne	6
Eremias	2	Discoglossus	12
Amphisbaena	2	Xenopus	6
Urosaurus	2	Litoria	3
Elgaria	1	Limnodynastes	3
Paroedura	1	Pelobates	30
Zonosaurus	1	Triturus	22
Furcifer	1	Alytes	2
Callisaurus	1	Bombina	5
Ameiva	3	Eupsophus	1
Sauromalus	1	Lechriodus	1
Aristelliger	1	Ceratophrys	2
Sphaerodactylus	1	Leptodactylus	3
		Leiopelma	3
		Eleutherodactylus	7
		Desmognathus	7
		Eurycea	1
		Chioglossa	1
		Laliostoma	1
		Ptychadena	1
		Scaphiophryne	1
		Rhacophorus	1
		Dicamptodon	1
		Lissotriton	5
		Mertensiella	1